

Optical study on incommensurate phase transitions of $(\text{C}_3\text{H}_7\text{NH}_3)_2\text{MnCl}_4$

K. Saito and J. Kobayashi

Kagami Memorial Laboratory for Material Science and Technology, Waseda University, 2-8-26, Nishiwaseda, Shinjuku-ku, Tokyo 169, Japan

(Received 5 September 1991)

The optical activity and birefringence of $(\text{C}_3\text{H}_7\text{NH}_3)_2\text{MnCl}_4$ were measured with use of the high-accuracy universal polarimeter (HAUP) method. An important property manifested by the incommensurate γ phase, i.e., reentrant phase transition, was studied in light of the knowledge that the optical gyration directly reflects the order parameter of the incommensurate modulation. Critical exponents β for the temperature variations of gyration in both high- and low-temperature regions of the γ phase were found to be nearly constant. Meanwhile, it is known that the values of critical exponents β of several A_2BX_4 -type incommensurate crystals are also in the same range ~ 0.42 – 0.47 , as determined by our recent HAUP experiments. These facts indicate that the incommensurately modulating waves of the γ phase appear as a helical phason mode and the γ phase reenters into a single phase accompanying two transitions of the same mechanism.

I. INTRODUCTION

Bis-propylammonium tetrachloromanganate $(\text{C}_3\text{H}_7\text{NH}_3)_2\text{MnCl}_4$ (abbreviated hereafter as PAMC) belongs to a general family $(\text{C}_n\text{H}_{2n+1}\text{NH}_3)_2\text{MX}_4$ with $M = \text{Mn, Cd, Fe, Cu, Cr, and Pd}$, and $X = \text{Cl and Br}$. The detailed structure of this crystal was analyzed by x-ray and neutron diffraction.^{1–3} A special feature of the structure of PAMC is that it contains two-dimensional perovskite layers consisting of corner-sharing MnCl_6^{2-} octahedra.¹ The layers are sandwiched by long propylammonium chains. The chains attach nearly normally to the layers through hydrogen bonds between the NH_3 groups and the chlorine ions.

PAMC has attracted much interest because of the following unique physical properties. (1) It undergoes five phase transitions from 169°C down to -155°C .² (2) Among six different phases in this temperature range, two phases defined as γ (Refs. 2 and 4) and ϵ (Refs. 5 and 6) appear through unusual incommensurate phase transitions which were not found in the other “normal” incommensurate crystals.

One of the most important phenomena in PAMC is that the phase transition of the γ phase was reported to be of the reentrant type.^{2,4} Muralt *et al.*⁴ pointed out that the amplitude of the incommensurately modulating wave in the γ phase would increase with decreasing temperature but vanish when it transformed into the commensurate phase without continuing to increase beyond the transition as is always found in normal incommensurate crystals. The symmetries of the two phases reentered by the γ phase therefore should be the same. They tried to explain the reason for the appearance of this transition by allowing for the coupling of the incommensurate order parameter with the interlayer distance of the perovskite layers. However, it seems to us that the agreement between theory and experiment was not perfect.

On the other hand, our high-accuracy universal polarimeter (HAUP) method^{7,8} revealed that the normal incommensurate phases of most A_2BX_4 crystals were optically active.^{9–11} We ascribed the origin of this phenomenon to the existence of a helically modulated wave in an incommensurate phase.¹² As a result it was proposed¹² that the strength of the optical activity is proportional to the amplitude of the modulated waves. In other words, optical activity can be a novel means for evaluating the amplitude of a modulated wave, and furthermore, for obtaining the soliton density n_s which had only been done by magnetic resonance methods.^{13–15} As a matter of fact, the temperature dependence of n_s of $[\text{N}(\text{CH}_3)_4]_2\text{CuCl}_4$ was successfully deduced by measuring a gyration tensor component.¹¹

We felt it worthwhile to reexamine peculiar incommensurate characteristics of PAMC by using the HAUP method. This paper reports some of the results.

II. EXPERIMENT

A part of the phase diagram of PAMC is shown in Fig. 1, where names and space groups, when known, are indicated to each phase.^{2,5,6} The symmetries of the β and δ phases are taken to be the same; the lattice parameters at room temperature are $a = 7.51 \text{ \AA}$, $b = 7.29 \text{ \AA}$, and $c = 25.94 \text{ \AA}$.¹

The original crystals were grown from aqueous solutions of $\text{C}_3\text{H}_7\text{NH}_2\text{HCl}$ and MnCl_4 by the temperature-decreasing method. For removing impurities, a recrystallization process was repeated three times. A crystal selected from the final output was cleaved into a (001) surface specimen with an area of about $1.2 \times 1.1 \text{ mm}^2$ and $7.3 \times 10^{-2} \text{ mm}$ thick. The specimen was subjected to the HAUP method where a light beam from a He-Ne laser struck the surface of the specimen at normal incidence. The temperature of the specimen was controlled within an error of $\pm 0.1^\circ\text{C}$ in all the temperature ranges

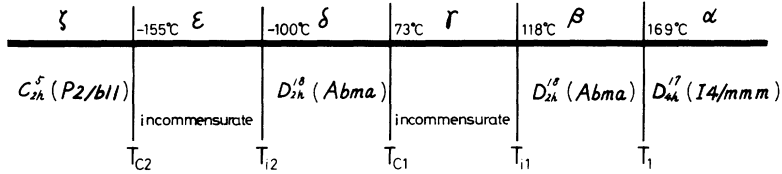


FIG. 1. Phase diagram of $(C_3H_7NH_3)_2MnCl_4$.

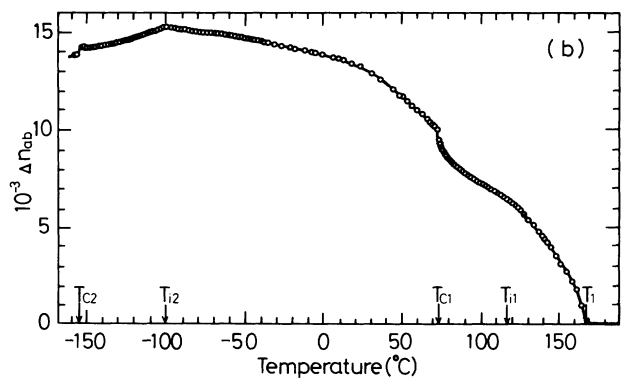
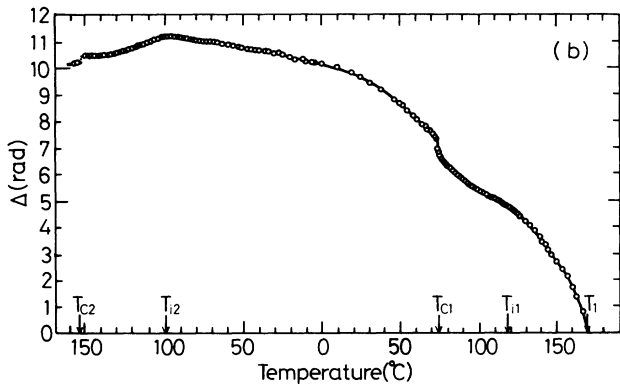
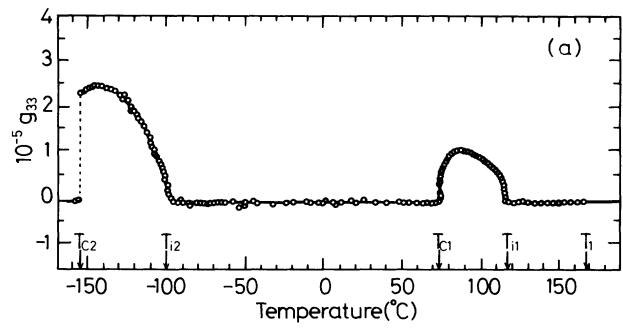
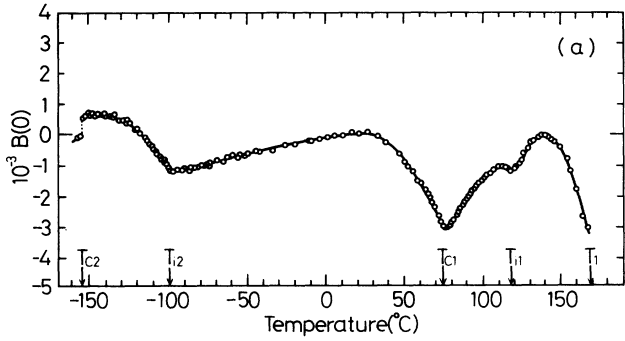


FIG. 2. Temperature dependences of $B(0)$ (a) and Δ (b) of $(C_3H_7NH_3)_2MnCl_4$.

FIG. 4. Temperature dependences of g_{33} (a) and Δn_{ab} (b) of $(C_3H_7NH_3)_2MnCl_4$.

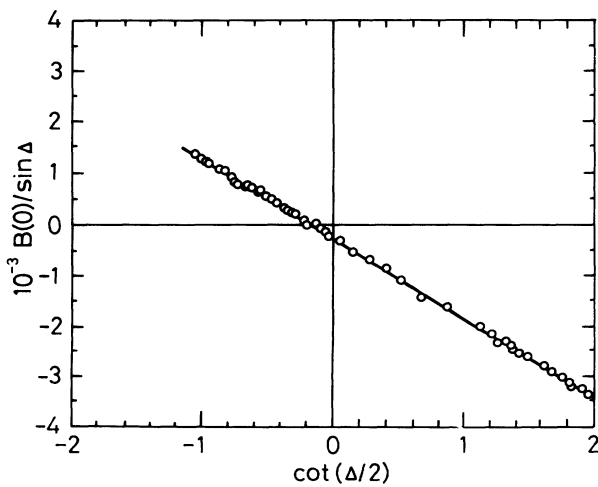


FIG. 3. Relationship between $B(0)/\sin\Delta$ and $\cot(\Delta/2)$ of $(C_3H_7NH_3)_2MnCl_4$.

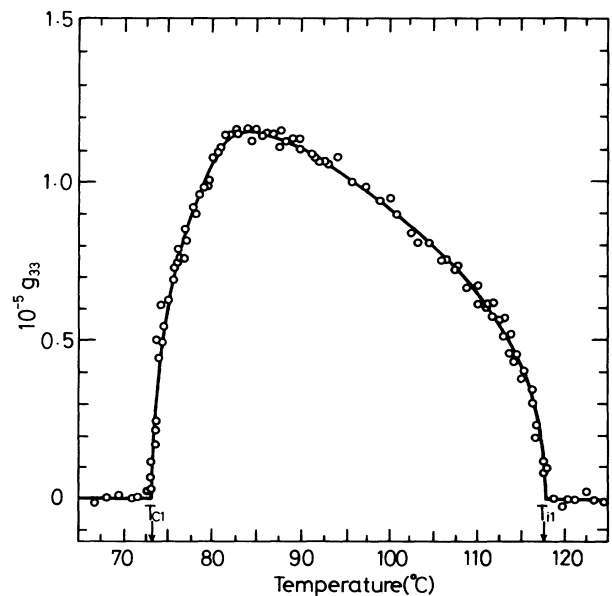


FIG. 5. Temperature dependence of g_{33} in the γ phase of $(C_3H_7NH_3)_2MnCl_4$.

tested.

The temperature dependence of $B(0)$ and Δ is shown in Figs. 2(a) and 2(b). As the δ phase is optically inactive, it was possible to determine the two systematic errors⁸ $\delta\Upsilon$ and γ by using the following equation:

$$B(0)/\sin\Delta = \gamma + \delta\Upsilon \cot(\Delta/2). \quad (1)$$

The relation between $B(0)/\sin\Delta$ and $\cot(\Delta/2)$ is shown in Fig. 3. As linearity was closely held, the errors could be evaluated as $\gamma = -2.84 \times 10^{-4}$ and $\delta\Upsilon = -1.52 \times 10^{-3}$. Using these values, temperature dependences of the gyration tensor component g_{33} and birefringence Δn_{ab} were determined in a temperature range between -170°C and 170°C . In the α phase above T_1 , the relative intensity Γ of the transmitted light through the specimen, which was placed between the crossed Nicols, was found to be extremely small, $\sim 10^{-7}$; furthermore, it was unchanged by the rotation of the specimen. Thus it was known that g_{33} and Δn_{ab} of the α phase are zero. They are indicated in Figs. 4(a) and 4(b), respectively. As seen in Fig. 4(a), the γ and ϵ phases are clearly optically active and the others are not. According to Fig. 4(b), Δn_{ab} exhibits characteristic anomalies at each transition point. The present optical data accords with the reported space groups of the relevant phases.

III. INCOMMENSURATE PHASE TRANSITIONS

The incommensurate phase transitions of the γ and ϵ phases will be discussed using the results shown in Fig. 4.

A. γ phase

The incommensurate modulation of the γ phase takes place along the a axis and its wave number is expressed as $(\frac{1}{6} + \delta)a^* + c^*$,² where the irrational fraction δ was reported to be almost independent of temperature.¹⁶ The temperature variation of g_{33} of this phase is depicted in detail in Fig. 5; g_{33} appears at $T_{i1} = 118^\circ\text{C}$, increases with the decrease of temperature, peaks at 83°C , then decreases rapidly and vanishes at $T_{c1} = 73^\circ\text{C}$.

We showed theoretically that a condensed complex order parameter manifests itself as a rotating helix with constant angular velocity.¹² This is the real entity of the phason mode in an incommensurate state and renders it optically active. Thus the observed gyration should be proportional to the radius of the helical mode which modulates existing lattice periods incommensurately.

Muralt *et al.*⁴ regarded the tilting angle of a propylammonium chain away from the layer normal as the primary order parameter η . η can be considered as complex, therefore it will be a natural consequence to assume that the aforementioned helical phason mode appears in the γ phase with a radius proportional to $|\eta|$. Then the observed gyration will be proportional to it. Accordingly, g_{33} in the higher-temperature region should depend on T in a form

$$g_{33} = M'_1 \left[\frac{T_{i1} - T}{T_{i1} - T_{c1}} \right]^{\beta_1} = M'_1 T_{R1}^{\beta_1}, \quad (2)$$

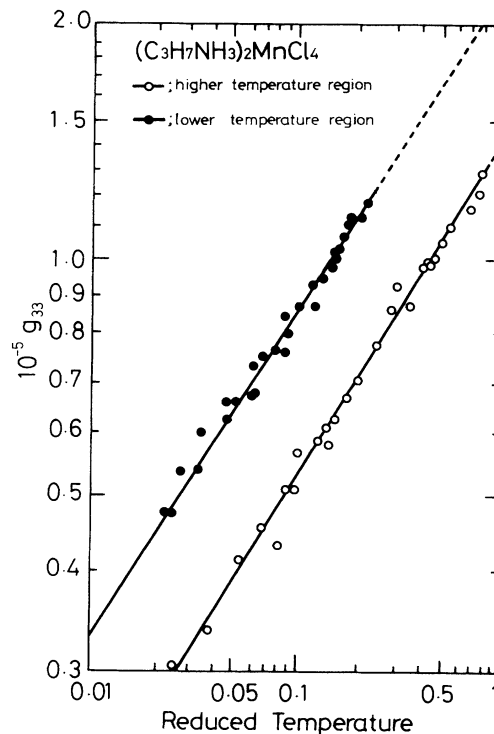


FIG. 6. Logarithmic plot of g_{33} vs reduced temperature in the γ phase of $(\text{C}_3\text{H}_7\text{NH}_3)_2\text{MnCl}_4$. The open circles indicate g_{33} in the higher-temperature region and the solid circles indicate g_{33} in the lower-temperature region.

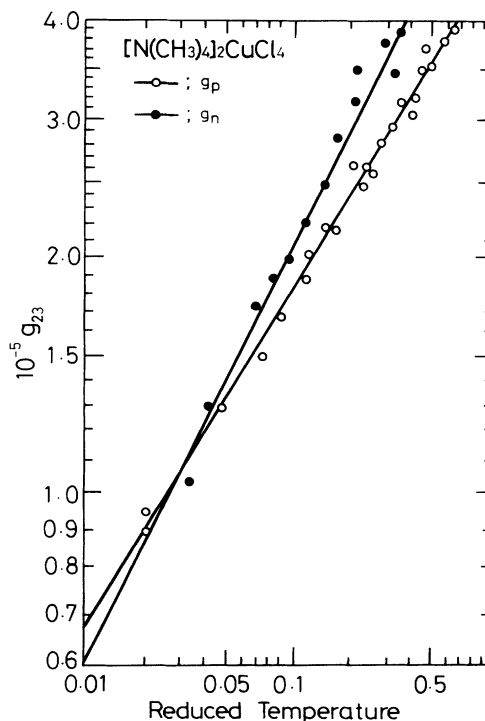


FIG. 7. Logarithmic plot of g_{23} vs reduced temperature of $[\text{N}(\text{CH}_3)_4]_2\text{CuCl}_4$. The open circles indicate g_p and the solid circles g_n .

TABLE I. Critical exponents of $(C_3H_7NH_3)_2MnCl_4$ and A_2BX_4 crystals.

Substance	Critical exponent	Reference
$[N(CH_3)_4]_2CuCl_4$	0.43	11
$[N(CH_3)_4]_2ZnCl_4$	0.42	9
Rb_2ZnCl_4	0.43	10
Rb_2ZnBr_4	0.42	17
$(NH_4)_2BeF_4$	0.47	17
$(C_3H_7NH_3)_2MnCl_4$		Present work
γ phase (higher-temperature region)	0.44	
(lower-temperature region)	0.42	
ϵ phase	0.46	

reflecting the scaling law of $|\eta|$. Here T_{R_1} expresses a reduced temperature, and M'_1 a constant. The observed values of g_{33} are plotted with respect to T_{R_1} on a logarithmic scale in Fig. 6. A linear relation is closely held between the quantities; the critical exponent being determined as $\beta_1=0.44$, with $M'_1=1.4 \times 10^{-5}$.

According to Murali *et al.*,⁴ one assumes that on the lower temperature side, $|\eta|$ decreases with decreasing temperature and becomes zero at T_{c1} . In this case, the corresponding equation to (2) must be

$$g_{33} = M'_2 \left[\frac{T - T_{c1}}{T_{i1} - T_{c1}} \right]^{\beta_2} = M'_2 T_{R_2}^{\beta_2}. \quad (3)$$

When the same plot as in the higher-temperature region was made, it displayed, as is also shown in Fig. 6, a parallel line to the former, providing $\beta_2=0.42$ with $M'_2=2.3 \times 10^{-5}$. Both critical exponents were found to almost coincide. It means that the correlation lengths of the fluctuation increase in the same way in the two events when the temperature approaches both T_{i1} and T_{c1} . This can be conceived as evidence that the mechanisms of the two transitions are identical. Thus the present experi-

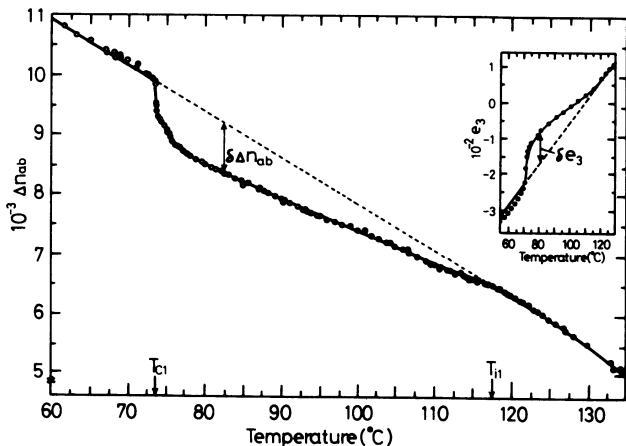


FIG. 8. Temperature dependence of Δn_{ab} in the γ phase of $(C_3H_7NH_3)_2MnCl_4$. The inset depicts the temperature dependence of the interlayer strain ϵ_3 measured by Murali *et al.* (Ref. 4).

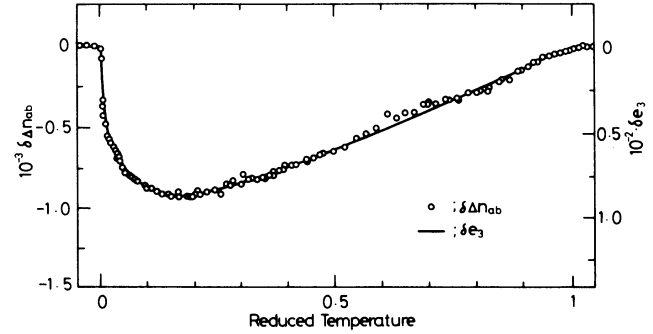


FIG. 9. Comparison of $\delta\Delta n_{ab}$ with $\delta\epsilon_3$ in the γ phase of $(C_3H_7NH_3)_2MnCl_4$.

ment strongly suggests that the incommensurate phase γ is embedded in a parent phase of the crystal, and in other words, it appears through the reentrant transition.

Critical exponents β of PAMC are compared with those of several normal A_2BX_4 crystals in Table I, where it must be noted that the data of A_2BX_4 crystals were obtained by measurements of optical activity.^{9-11,17} It is significant that β of all the crystals listed are confined to nearly constant values, ca. 0.42-0.47. This fact supports our assumption that the modulation wave of PAMC appears as a helical phason mode as were the cases in A_2BX_4 crystals.

In a normal A_2BX_4 crystal, the magnitude of the amplitude mode, viz., the radius of the helix increases with decreasing temperature. The anisotropy energy of the crystal gradually prevails, and the helical structure begins to collapse. The crystal is segregated into soliton and domain regions, and undergoes a lock-in transition to the commensurate phase at last. This transition can be looked upon conversely as one where the soliton density develops in the incommensurate phase as an order parameter.¹⁸ Therefore it is of interest to examine the scaling law of the temperature dependence of the soliton density. In Fig. 7 logarithmic plots of a gyration component g_p (Ref. 11) due to the phason, and g_n due to the soliton of g_{23} of $[N(CH_3)_4]_2CuCl_4$ are made with regards to the reduced temperature. The critical exponents are obtained as $\beta_p=0.43$ with $M_p=5.0 \times 10^{-5}$ for the former, and $\beta_n=0.53$ with $M_n=6.7 \times 10^{-5}$ for the latter. β_p falls in the aforementioned constant region as expected but β_n deviates from it. These facts also support our previous conclusion on the reentrant phase transition.

The temperature change of Δn_{ab} of the γ phase is

TABLE II. Elasto-optic coefficients of $(C_3H_7NH_3)_2MnCl_4$ and some dielectric crystals.

Substance	p	Reference
KH_2PO_4	$p_{11}=2.5 \times 10^{-1}$	23
α -quartz	$p_{11}=1.4 \times 10^{-1}$	24
$LiNbO_3$	$p_{11}=2.5 \times 10^{-2}$	25
$LiTaO_3$	$p_{11}=8.0 \times 10^{-2}$	23
$(C_3H_7NH_3)_2MnCl_4$	$p_{13}-p_{23}=4.8 \times 10^{-2}$	Present work

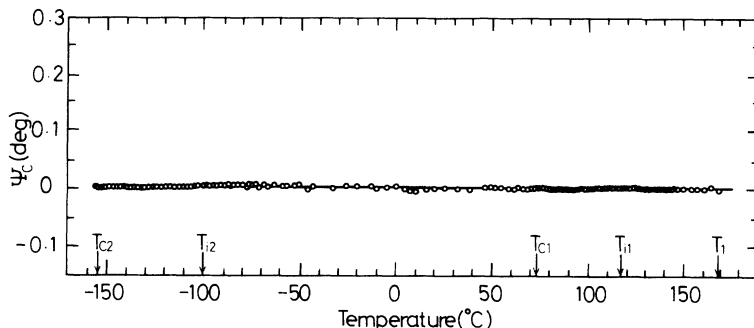


FIG. 10. Temperature dependence of the rotation angle ψ_c of the indicatrix of $(C_3H_7NH_3)_2MnCl_4$ around the c axis.

represented in detail in Fig. 8. It is clearly seen in the figure that the straight extension of Δn_{ab} of the β phase connects with that of the δ phase. This is consistent with the fact that the symmetries of both phases are the same. The temperature change of Δn_{ab} of PAMC was already measured by Brunskill and Depmeier,¹⁹ Schäfer and Kleemann,²⁰ and Mintegua *et al.*,²¹ but this point was not clearly observed by Brunskill and Depmeier and Schäfer and Kleemann, but it was by Mintegua *et al.* Δn_{ab} of the γ phase is definitely deflected from the above-mentioned line between T_{i1} and T_{c1} . The corresponding behavior of the interlayer strain e_3 was measured by Muralt *et al.*⁴ as shown in the inset in Fig. 8. It is found that the temperature dependences of the optical and mechanical distortions, $\delta(\Delta n_{ab})$ and δe_3 , in the γ phase perfectly coincide as seen in Fig. 9.

It is possible to determine an elasto-optic coefficient p_{ij} from the relation of Fig. 9. Using the dielectric imper-

meability tensor B_i ,

$$B_i = \delta \left[\frac{1}{n_i^2} \right] = p_{i3} e_3 . \tag{4}$$

It must be noted that as the γ phase is in an incommensurate state its space group cannot be assigned to any of the three-dimensional ones.²² Our HAUP test provided evidence that the rotation angle ψ_c of the indicatrix around the c axis was always zero as indicated in Fig. 10. Therefore it is certain that $p_{43} = p_{53} = p_{63} = 0$ in the γ phase. Then the equation of the indicatrix is written as

$$\left[\frac{1}{n_1^2} + p_{13} e_3 \right] x^2 + \left[\frac{1}{n_2^2} + p_{23} e_3 \right] y^2 + \left[\frac{1}{n_3^2} + p_{33} e_3 \right] z^2 = 1 . \tag{5}$$

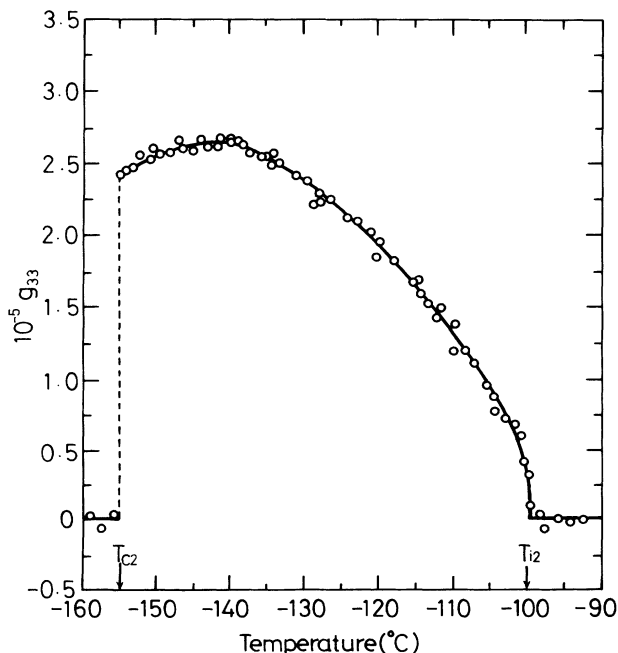


FIG. 11. Temperature dependence of g_{33} in the ϵ phase of $(C_3H_7NH_3)_2MnCl_4$.

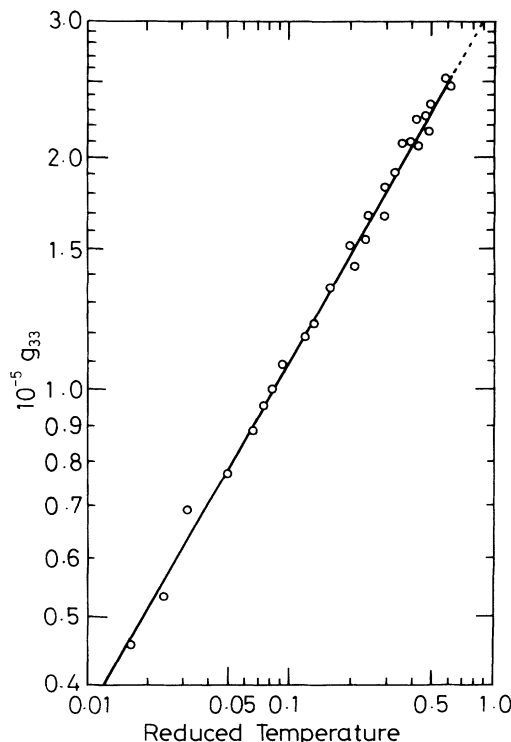


FIG. 12. Logarithmic plot of g_{33} vs reduced temperature in the ϵ phase of $(C_3H_7NH_3)_2MnCl_4$.

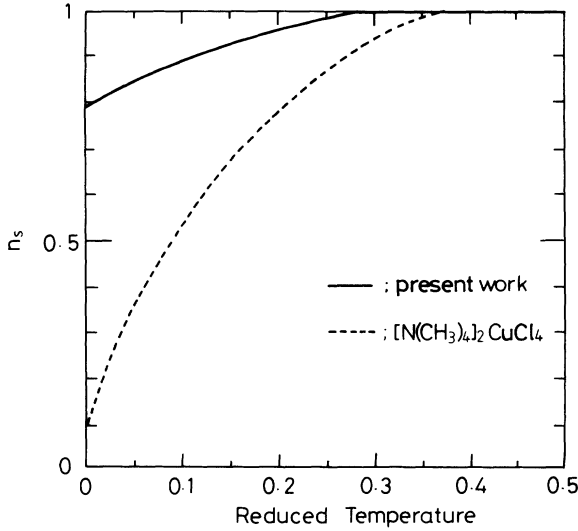


FIG. 13. Expected behavior of n_s in the ϵ phase of $(C_3H_7NH_3)_2MnCl_4$ plotted with respect to the reduced temperature (see text). n_s of $[N(CH_3)_4]_2CuCl_4$ is also depicted by the dashed line for the sake of comparison.

From this equation the principal refractive indices are derived as

$$n_1 = n_1^0 - \frac{1}{2}n_1^0 p_{13} e_3, \quad (6a)$$

$$n_2 = n_2^0 - \frac{1}{2}n_2^0 p_{23} e_3, \quad (6b)$$

and

$$n_3 = n_3^0 - \frac{1}{2}n_3^0 p_{33} e_3, \quad (6c)$$

where n_1^0 , n_2^0 and n_3^0 are original refractive indices along the crystallographic a , b , and c axes. Therefore the change of birefringence $\delta(\Delta n_{ab})$ viewed from the c axis is expressed by

$$\delta(\Delta n_{ab}) = -\frac{1}{2}(n_1^0 p_{13} - n_2^0 p_{23})e_3. \quad (7)$$

By using the values in Fig. 9, it was obtained that $p_{13} - p_{23} = 4.8 \times 10^{-2}$. This value was compared with elasto-optic coefficients of other crystals in Table II, and was found to range in the ordinary order.

B. ϵ phase

The detailed representation of the temperature dependence of g_{33} of the ϵ phase of PAMC is given in Fig. 11. It appears suddenly at $T_{i2} = -100^\circ\text{C}$, after peaking at about -140°C , decreases, and vanishes with a large discontinuity at $T_{c2} = -155^\circ\text{C}$. The logarithmic plot of g_{33} against reduced temperature, shown in Fig. 12, provides $\beta = 0.46$ with $M = 3.3 \times 10^{-5}$. Judging from this value, this transition should be of the phason type as expected. Unfortunately it was not possible to determine the critical exponent for the transition to the ζ phase, because the temperature range was so narrow and terminated by the severely discontinuous transition.

The lock-in transition of the ϵ phase was reported to be peculiar in that the incommensurate wave vector $(\frac{1}{3} + \delta)b^*$ switches to a commensurate value of $\frac{1}{3}(b^* \pm c^*)$,⁶ instead of a triplication along the b^* axis. Besides, it has not yet been clarified whether or not the structure of the domains in the incommensurate phase is the same as that of the ζ phase. Our experimental result only suggested that the domains were likely to be optically inactive. The temperature dependence of n_s was deduced from present measurements by assuming that the domains are really optically inactive. It is shown in Fig. 13 where n_s of $[N(CH_3)_4]_2CuCl_4$ is also depicted for the sake of comparison.

The temperature dependence of Δn_{ab} shown in Fig. 14 is in qualitative agreement with the reports of Brunskill and Depmeier,¹⁹ Schäfer and Kleemann,²⁰ and Minteguia *et al.*²¹ An elasto-optic coefficient was derived using the data of strains e_3 given by Minteguia *et al.*²¹: $p_{13} - p_{23} = -8.7 \times 10^{-2}$. The magnitude is approximately the same as that of the γ phase, but the sign is reversed. This discrepancy is not understood.

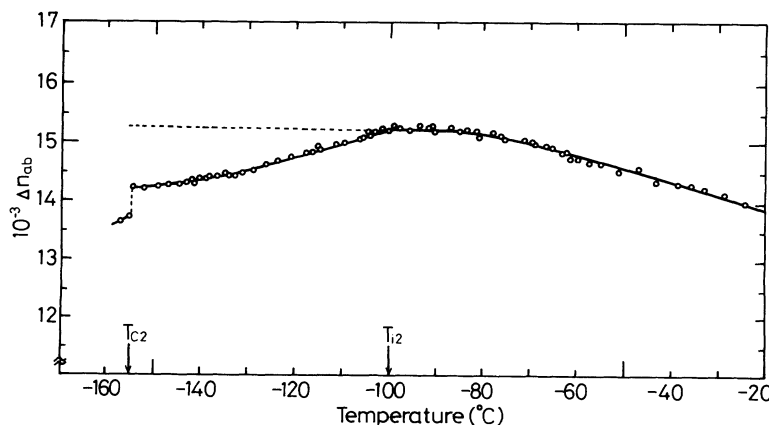


FIG. 14. Temperature dependence of Δn_{ab} in the ϵ phase of $(C_3H_7NH_3)_2MnCl_4$.

IV. DISCUSSIONS

Muralt *et al.*⁴ developed a phenomenological theory of PAMC for explaining the reentrant transition of the γ phase. They introduced a coupling term into the free energy of the system; it connects the order parameter η with a second-order parameter which represents a non-symmetry breaking interlayer distance d of the MnCl_6^{2-} layer. The theory accounted for an incommensurate phase in an interval of T_{i1} and T_{c1} , where not only $|\eta|$ but also d are modulated. In a word, there exists an optimum interval of d for the incommensurate modulation to exist.

They deduced the temperature dependence of $|\eta|$ through the best fit of the observed strains δe_3 with the theory.^{4,26} The result is depicted in Fig. 15, where the directly observed order parameters $\Delta\rho$ from NMR spectroscopy²⁶ are indicated for the sake of comparison. It appears that the coincidence of the theoretical curve with the observed values is not perfect. In the same figure our result of optical gyrations is indicated. It agrees fairly well with the theoretical curve. It has already been argued that a close agreement exists in the temperature dependences of their δe_3 and our $\delta(\Delta n_{ab})$ measurements. Then it will be concluded that their theory explains the truth of the reentrant transition of this crystal and our gyration experiment reflects the order parameter more faithfully than the NMR method. A slight disagreement between gyrations and the theoretical curve in a limited temperature range might indicate the appearance of soliton regions in this range.

Minteguia *et al.*²¹ claimed that the theory of Muralt *et al.*⁴ was not the only possible explanation for a reentrant behavior that can be conceived in the framework of

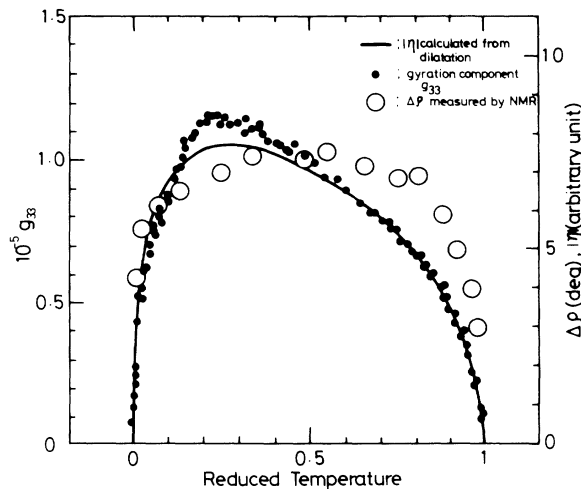


FIG. 15. Comparison of the theoretical and observed order parameters of the γ phase of $(\text{C}_3\text{H}_7\text{NH}_3)_2\text{MnCl}_4$.

Landau theory. They stressed the coupling of two order parameters corresponding to the β and γ phases which developed from a common parent α phase. However, the result of the temperature dependence of $|\eta|$ was the same as that of Muralt *et al.* Therefore the essential difference of the theories could not be detected by the present experiment.

ACKNOWLEDGMENT

The authors thank Mr. Y. Suga for his help in the present experiment.

¹E. R. Peterson and R. D. Willett, *J. Chem. Phys.* **56**, 1879 (1972).

²W. Depmeier, J. Felsche, and G. Wildermuth, *J. Solid State Chem.* **21**, 57 (1977).

³W. Depmeier and S. A. Mason, *Acta Crystallogr. Sect. B* **34**, 920 (1978).

⁴P. Muralt, R. Kind, R. Blinc, and B. Zeks, *Phys. Rev. Lett.* **49**, 1019 (1982).

⁵W. Depmeier and S. A. Mason, *Solid State Commun.* **44**, 719 (1982).

⁶W. Depmeier and S. A. Mason, *Solid State Commun.* **46**, 409 (1983).

⁷J. Kobayashi and Y. Uesu, *J. Appl. Crystallogr.* **16**, 204 (1983).

⁸J. Kobayashi, H. Kumomi, and K. Saito, *J. Appl. Crystallogr.* **19**, 377 (1986).

⁹J. Kobayashi and K. Saito, *Proc. Jpn. Acad.* **62**, 177 (1986).

¹⁰J. Kobayashi, K. Saito, H. Fukase, and K. Matsuda, *Phase Transitions* **12**, 225 (1988).

¹¹K. Saito, H. Sugiya, and J. Kobayashi, *J. Appl. Phys.* **68**, 732 (1990).

¹²J. Kobayashi, *Phys. Rev. B* **42**, 8332 (1990).

¹³R. Blinc, V. Rutar, B. Topic, F. Milia, J. P. Aleksandrova, A.

S. Chavas, and R. Gazzinelli, *Phys. Rev. Lett.* **46**, 1406 (1981).

¹⁴R. Blinc, B. Lozar, F. Milia, and R. Kind, *J. Phys. C* **17**, 24 (1984).

¹⁵R. Blinc, V. Rutar, B. Topic, F. Milia, and Th. Rashing, *Phys. Rev. B* **33**, 1721 (1986).

¹⁶W. Depmeier, *Solid State Commun.* **45**, 1089 (1983).

¹⁷K. Saito and J. Kobayashi (unpublished).

¹⁸P. Prelovsek and R. Blinc, *J. Phys. C* **17**, 577 (1984).

¹⁹I. H. Brunskill and W. Depmeier, *Acta Crystallogr. Sect. A* **38**, 132 (1982).

²⁰F. J. Schäfer and W. Kleemann, *Ferroelectrics* **55**, 163 (1984).

²¹R. C. Minteguia, M. J. Tello, J. M. Perez-Mato, A. Gomez-Cuevas, and J. Fernandez, *Solid State Commun.* **50**, 501 (1984).

²²A. Janner and T. Janssen, *Phys. Rev. B* **15**, 643 (1977).

²³R. W. Dixon, *J. Appl. Phys.* **38**, 5149 (1967).

²⁴F. Pockels, *Ann. Phys. Chem.* **37**, 144 (1889).

²⁵V. V. Lemanov, O. V. Shakin, and G. A. Smolenskii, *Fiz. Tverd. Tela (Leningrad)* **13**, 533 (1971) [*Sov. Phys. Solid State* **13**, 426 (1971)].

²⁶P. Muralt, *J. Phys. C* **19**, 1689 (1986).